

## Estimation of Non-Linear Fracture Parameter Using Enhanced Reference Stress Method

300

J- ( C\*)

J C\*

### Abstract

This paper provides the new engineering method, called the enhanced reference stress method, to estimate  $J$  (or  $C^*$ ) for non-linear fracture mechanics analysis of defective components. The proposed method offers significant advantages over existing methods in terms of its accuracy, simplicity and robustness. Examples of application of the proposed method to typical piping integrity problems such as through-wall cracked pipes and surface cracked pipes. Excellent agreements between the FE  $J$  and  $C^*$  results and those of the proposed method provide sufficient confidence in the use of the proposed method.

1.

1970 Rice<sup>1)</sup>가

J-

(Non-Linear Fracture Mechanics)

가 가 80

. 1980 (Electric Power Research Institute, GE/EPRI Handbook<sup>2-</sup>)

EPR1) (Central Electric Generating Board,

<sup>5)</sup> R6<sup>6)</sup> R5<sup>7)</sup>

가 <sup>8,9)</sup>가

SINTAP(Structural Integrity Assessment Procedures for European Industry)<sup>10)</sup>

<sup>11)</sup>

(J- C\* - ) 가

GE/EPRI (Reference stress method)

GE/EPRI J- ( C\* - )

, Ramberg-Osgood

가

3

가

) Ramberg-Osgood ( )

J- ( C\* - ) 가

GE/EPRI Ainsworth<sup>12)</sup>

<sup>13)</sup> 가 J- (

C\* - ) J- ( C\* - )

) J- ( C\* - )

가

가 가

(Enhanced Reference Stress Method)

2.

GE/EPRI

J-

6)

$$J_p = a \left( \frac{s_y^2}{E} \right) G \cdot h_1(n) \left[ \frac{P}{P_o} \right]^{n+1} \quad (1)$$

가  $s_y$ ,  $P_o$  (n),  $E$ , Young's Modulus, G,  $h_1$ , J-

$$J_e = \frac{K^2}{E'} = \left( \frac{s_y^2}{E} \right) G \cdot h_1(n=1) \left[ \frac{P}{P_o} \right]^2 \quad (2)$$

, K (plane strain)  $E'=E$  (1), (stress intensity factor)  $E'=E/(1-n^2)$  (plane stress)  $h_1(n=1)$  (n=1)  $h_1$  (2)

$$\frac{J_p}{J_e} = a \frac{h_1(n)}{h_1(n=1)} \left[ \frac{P}{P_o} \right]^{n-1} \quad (3)$$

(3)  $h_1(n)/h_1(n=1)$  가 (n)  $P_o$   $P_{ref}$

$$\frac{J_p}{J_e} = a \left\{ \frac{h_1(n)}{h_1(n=1)} \left[ \frac{P_{ref}}{P_o} \right]^{n-1} \right\} \left[ \frac{P}{P_{ref}} \right]^{n-1} \quad (4)$$

$h_1(n)/h_1(n=1)$   $P_{ref}/P_o$  가 (n)  $P_{ref}$  가 (n) (Optimized reference load),  $P_{oR}$  가 (4)

$$\frac{J_p}{J_e} \approx a \left[ \frac{P}{P_{oR}} \right]^{n-1} \quad (5)$$

(5) 가 Ramberg-Osgood 가

$$\frac{J_p}{J_e} \approx \frac{E \mathbf{e}_{ref}}{\mathbf{s}_{ref}} ; \mathbf{s}_{ref} = \frac{P}{P_{oR}} \mathbf{s}_y \quad (6)$$

$\mathbf{s} = \mathbf{s}_{ref}$  ,  $\mathbf{e}_{ref}$  (6) J-

$$\frac{J}{J_e} = \frac{E \mathbf{e}_{ref}}{\mathbf{s}_{ref}} + \frac{1}{2} \left( \frac{\mathbf{s}_{ref}}{\mathbf{s}_y} \right)^2 \frac{\mathbf{s}_{ref}}{E \mathbf{e}_{ref}} ; \mathbf{s}_{ref} = \frac{P}{P_{oR}} \mathbf{s}_y \quad (7)$$

(7)  $J_e$  GE/EPRI  $P_{oR}$  GE/EPRI  
 GE/EPRI 가  
 (Strain hardening exponent)

### 3.

#### 3.1 J-

Fig. 1 가 (P), (M), (p) (P<sub>oR</sub>)

$$\begin{aligned}
 P_{oR} &= \mathbf{g} \cdot P_L \quad ; \quad M_{oR} = \mathbf{g} \cdot M_L \\
 P_{oR} &= \mathbf{y} \cdot P_L
 \end{aligned}
 \tag{8}$$

,  $P_L$  ,  $M_L$  ,  $P_L$  .

$$P_L = 2R_m t s_y \left[ \mathbf{p} - \mathbf{q} - 2 \sin^{-1} \left( \frac{1}{2} \sin \mathbf{q} \right) \right] \tag{9}$$

$$M_L = 4R_m^2 t s_y \left[ \cos \left( \frac{\mathbf{q}}{2} \right) - \frac{1}{2} \sin \mathbf{q} \right] \tag{10}$$

$$P_L = \frac{2t}{pR_m} s_y \left[ \mathbf{p} - \mathbf{q} - 2 \sin^{-1} \left( \frac{1}{2} \sin \mathbf{q} \right) \right] \tag{11}$$

$$(8) \quad \mathbf{g} \cdot \mathbf{y}$$

$$\mathbf{g}(\mathbf{q}) = 0.82 + 0.75 \left( \frac{\mathbf{q}}{\mathbf{p}} \right) + 0.42 \left( \frac{\mathbf{q}}{\mathbf{p}} \right)^2 \tag{12}$$

$$\mathbf{y}(\mathbf{q}) = 0.45 + 1.88 \left( \frac{\mathbf{q}}{\mathbf{p}} \right) - 0.75 \left( \frac{\mathbf{q}}{\mathbf{p}} \right)^2 \tag{13}$$

.17)

$$\left( \frac{P}{P_{oR}} \right)^2 + \frac{M}{M_{oR}} = 1 \tag{14}$$

$P_{oR}$   $M_{oR}$  (8) . 가 가

$$\left( \frac{p}{P_{oR}} \right)^2 + \frac{M}{M_{oR}} = 1 \tag{15}$$

J- (J<sub>e</sub>)

R<sub>m</sub>/t 4.48 . 355.6mm, 35.7mm ,  
 TP304(50 ) TP316(288 ) ,  
 Fig. 2

1/4 , ABAQUS 18)  
 20 (20-nodes isoparametric brick  
 reduced integration element) 936 ,  
 (small strain analysis)

Fig. 3

J-  
 Fig. 4

Fig. 3, 4

J-

4.

가

J-

가

J-

J-

J-

4.1 J-

Fig. 5

가

(p), (M)가 ,  
 (p<sub>oR</sub>) (M<sub>oR</sub>)

$$p_{oR} = \mathbf{g} \cdot p_L \quad \text{for internal pressure}$$

$$\mathbf{g} = 1.767(a/t)(\mathbf{b}/\mathbf{p}) - 0.156(a/t) - 0.101(\mathbf{b}/\mathbf{p}) + 0.627 \quad (16)$$

$$M_{oR} = \mathbf{g} \cdot M_L \quad \text{for global bending}$$

$$\mathbf{g} = \mathbf{q}_1(a/t)^2 + \mathbf{q}_2(a/t) + 1.04$$

$$\mathbf{q}_1 = 4.26(\mathbf{b}/\mathbf{p})^2 - 1.35(\mathbf{b}/\mathbf{p}) + 0.80 \quad (17)$$

$$\mathbf{q}_2 = -2.30(\mathbf{b}/\mathbf{p})^2 - 1.57(\mathbf{b}/\mathbf{p}) - 0.77$$

$p_L$   $M_L$

$$p_L = \frac{2s_y t}{R_m} \left( 1 - \frac{ba/t + 2 \sin^{-1}[a \sin(b/2)/t]}{p} \right) \quad (18)$$

$$M_L = 4R_m^2 t s_y \left( \cos \left[ \frac{ab}{2t} \right] - \frac{a \sin b}{2t} \right) \quad (19)$$

가

$$J_e = J_e \quad (7)$$

$$(f=0, 5) \quad J$$

$$J_e \quad (7)$$

$J_e$

J

4.2

3, Fig. 6

Fig. 7 8

J-

J-

$$J_n = \frac{J}{s_y(t-a)(a/t)} \quad (20)$$

Fig. 7 8

J-

Fig.

9

J-

J-

5.

가

가

C\*

5.1 C\* -

C\* -

$$C^* = \left( \frac{K^2}{E'} \right) \frac{E \dot{\epsilon}_c}{s_{ref}} \quad (21)$$

$$s_{ref} \quad , \quad \dot{\epsilon}_c \quad s = s_{ref} \quad (21)$$

가

5.2

565°C CMV

RCC-MR law<sup>25)</sup>

q-projection law<sup>24)</sup>

TP316

Fig. 10 projection creep law

가

RCC-MR q-

Fig. 11

C\* -

6.

C\* -

J-

가

J-

C\* -



- 1) Rice, J.R., 1968, " A Path Independent Integral and the Approximated Analysis by Notches and Cracks " , Journal of Applied Mechanics, 35, pp. 379-386.
- 2) Kumar V, German D, Shih CF. An Engineering Approach for Elastic-Plastic Fracture Analysis. EPRI Final Report NP 1931, 1981.
- 3) Kumar V. Estimation Technique for the Prediction of Elastic-Plastic Fracture of Structural Components of Nuclear Systems. 5<sup>th</sup> and 6<sup>th</sup> Semi-annual Reports to EPRI, 1982.
- 4) Kumar, V. and German, M.D., 1998, Elastic-Plastic Fracture Analysis of Through-Wall and Surface Flaws in Cylinders, EPRI Report, NP-5596.
- 5) Zahoor, A., 1991, Ductile Fracture Handbook, Novotech Corp. 3 Volumes.
- 6) R6, 1999, R6: Assessment of the Integrity of Structures Containing Defects, Revision 3, Amendment 10, British Energy.
- 7) R5, 1998, R5: Assessment Procedure for the High Temperature Response of Structures, Issue 2, British Energy.
- 8) Wilkowski, G, et al., 1997, International Piping Integrity Research Group (IPIRG) Program Program Final Report. NUREG/CR-6233, USNRC.
- 9) Hopper, A, et al., 1997, The Second International Piping Integrity Research Group (IPIRG-2) Program Final Report. NUREG/CR-6452, USNRC, 1997.
- 10) Final Procedure: SINTAP (Structural Integrity Assessment Procedures for European Industry), Brite-Euram Project, BE95-1426, November 1999.
- 11) Anderson, T.L., 1995, Fracture Mechanics Fundamentals and Applications, CRC Press.
- 12) Ainsworth, R.A., 1984, " The Assessment of Defects in Structures of Strain Hardening Materials, " Engineering Fracture Mechanics, Vol. 19, pp. 633~642.
- 13) Penny R.K. and Marriot, D-L., 1995, Design for Creep, Chapman & Hall.
- 14) R66, 1999, AGR Materials Data Handbook, Issue 5. C D Hamm (ed.), British Energy Generation Ltd.

15) RCC-MR, 1985, Design and Construction Rules for Mechanical Components of FBR Nuclear Islands, AFCEN, Paris.

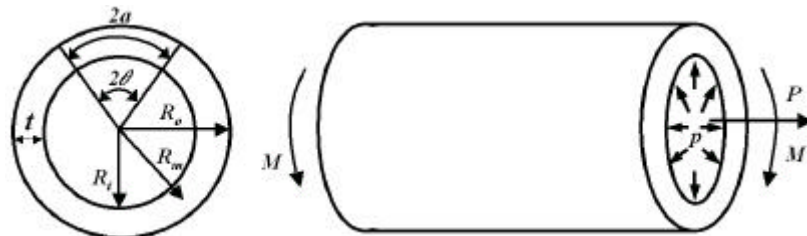


Fig. 1 Circumferential through-wall cracked pipes under axial tension (P), pure bending (M) and internal pressure (p).

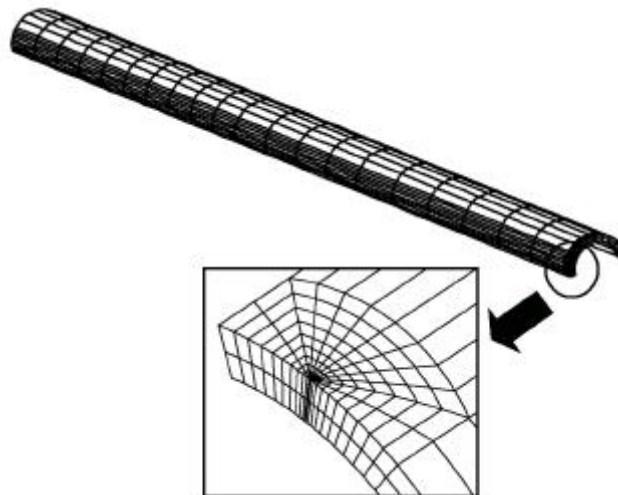
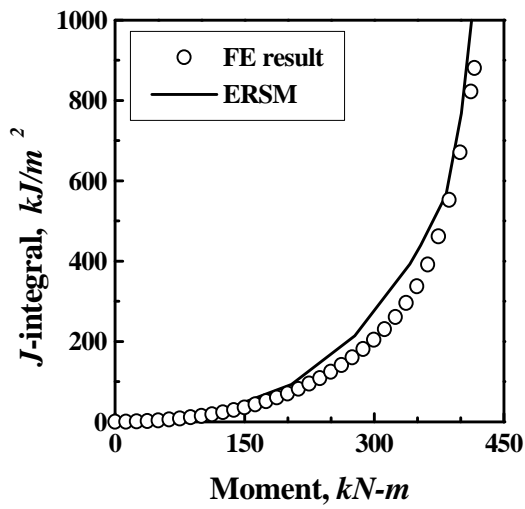
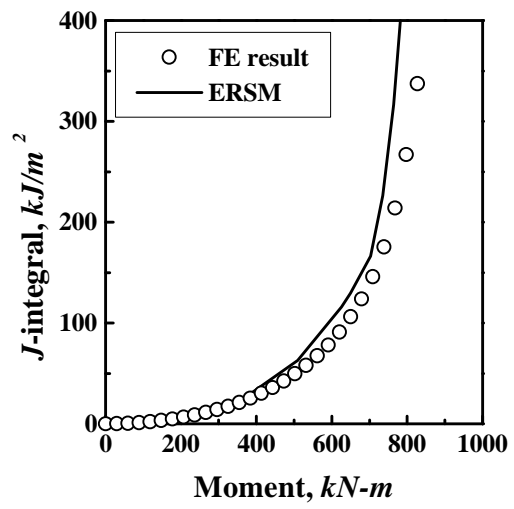


Fig. 2 A 3-D FE mesh for the circumferentially through-wall cracked pipe

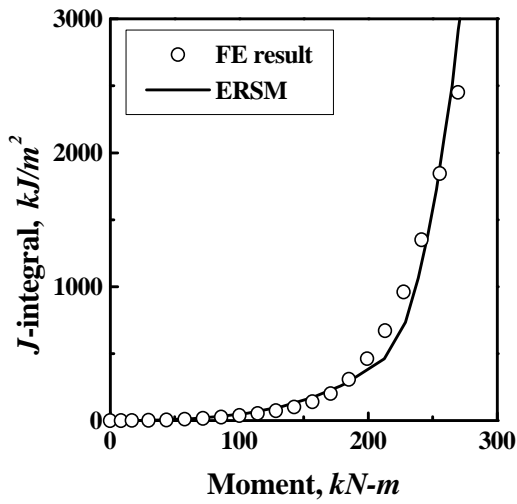


(a)

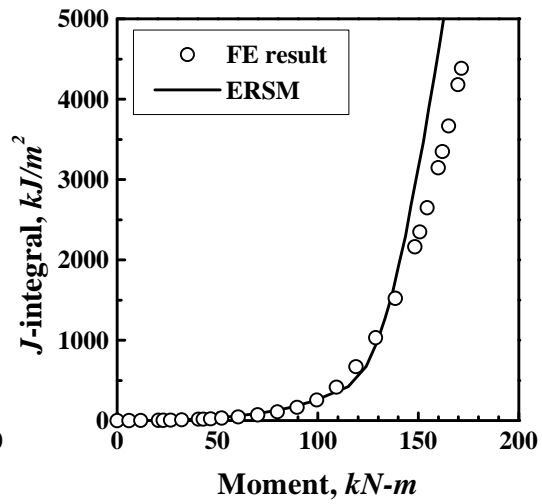


(b)

Fig. 3 Comparison of FE J values under pure bending with those of the proposed method for (a)  $q/p = 0.4$  and (a)  $q/p = 0.125$ .



(a)



(b)

(Continued)

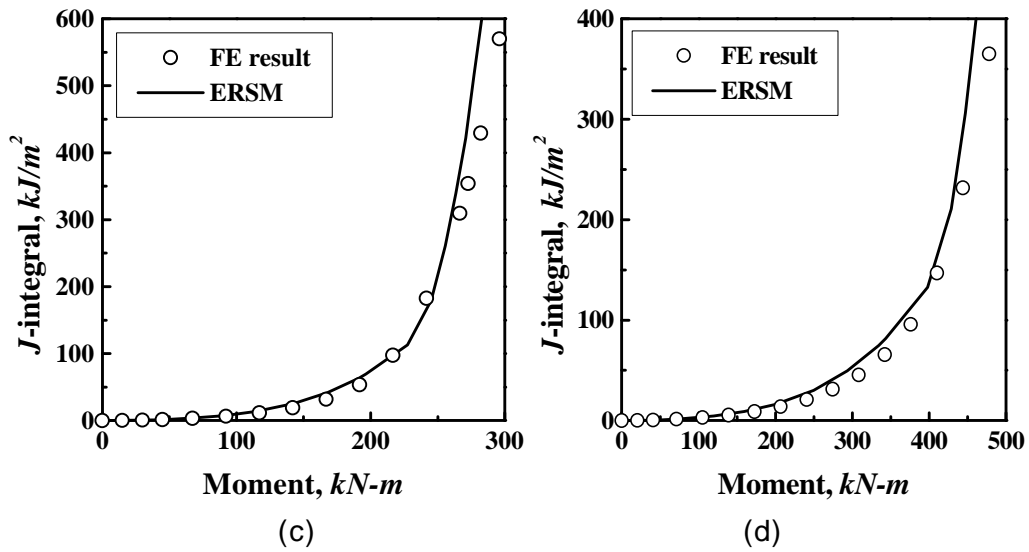


Fig. 4 Comparison of FE J values for combined bending and tension with those of the proposed method: for the load proportionality factor  $l=0.5$  (a)  $q/p=0.4$ , (b)  $q/p=0.125$ , for  $l=2.0$  (c)  $q/p=0.4$ , (d)  $q/p=0.125$ .

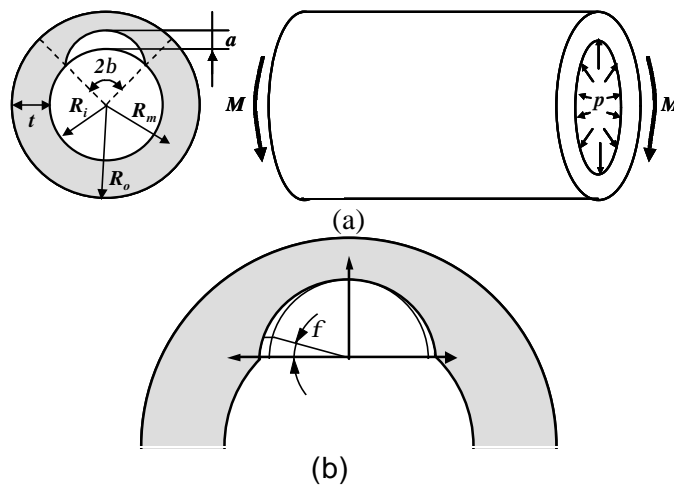


Fig. 5 (a) Schematic illustration for surface cracked pipes in internal pressure  $p$  and in global bending  $M$ , and (b) definition of the crack angle.

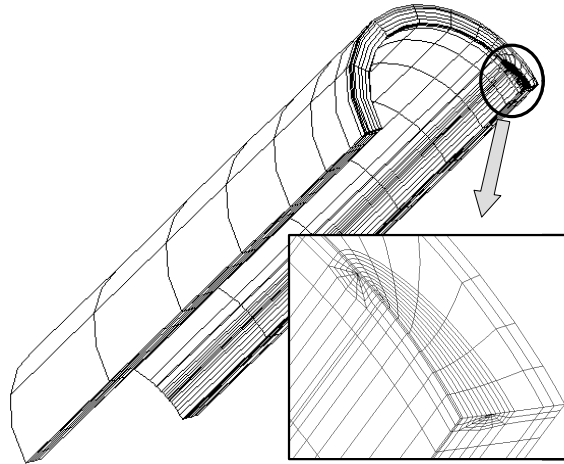


Fig. 6 A typical FE mesh for  $R_m/t=5$ ,  $a/t=0.3$  and  $b/p=0.1$ .

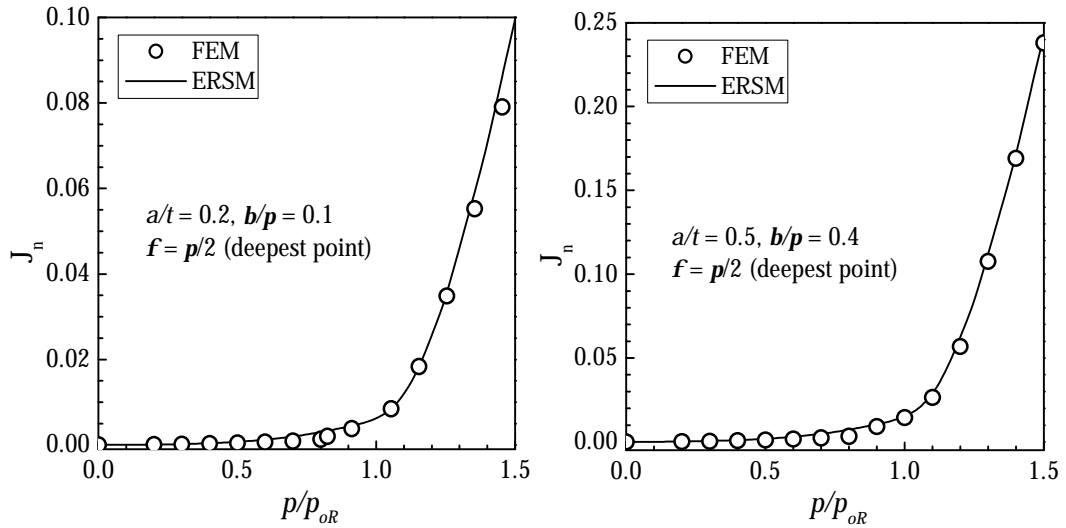


Fig. 7 Comparison of the FE  $J$  results with those from the proposed method under internal pressure.

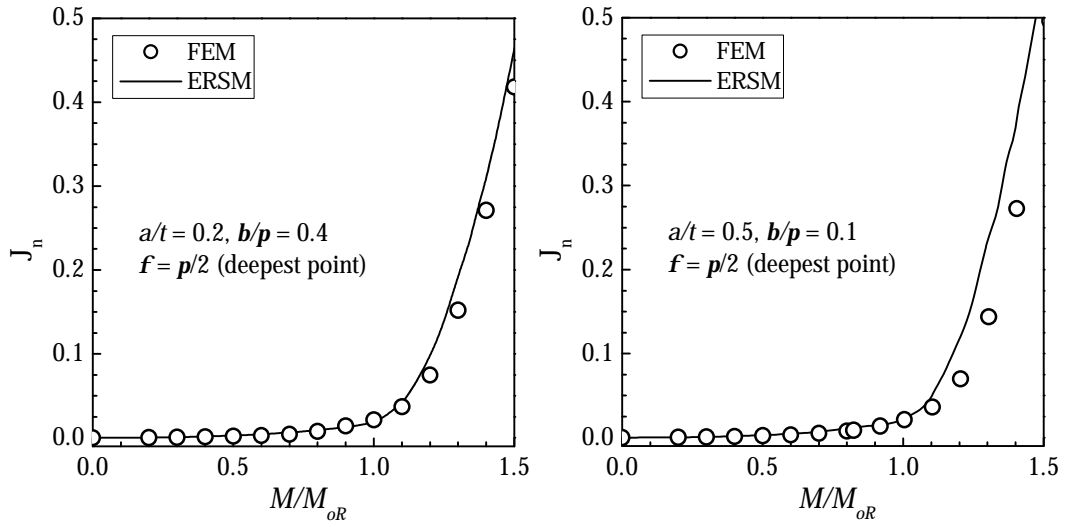


Fig. 8 Comparison of the FE  $J$  results with those from the proposed method under global bending.

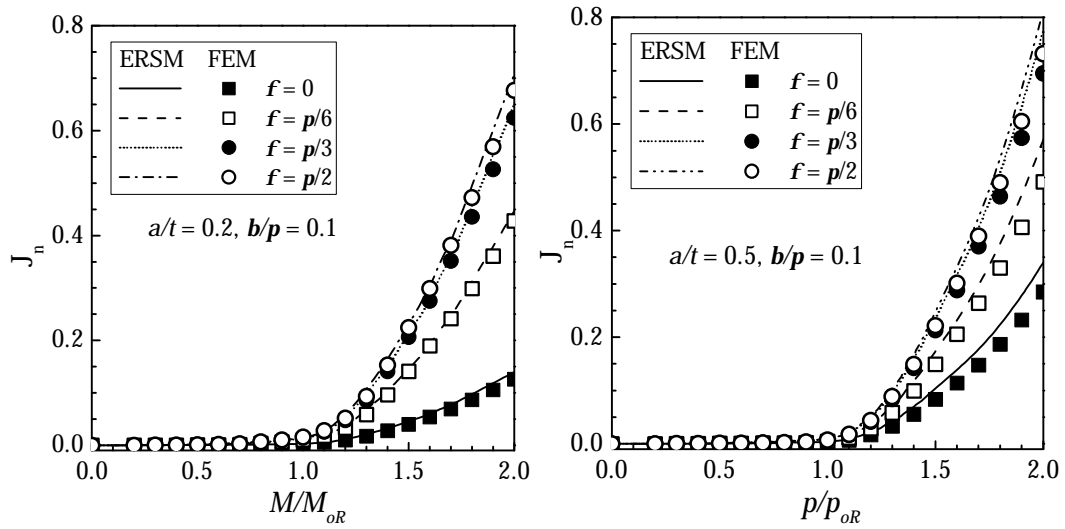


Fig. 9 Comparison of the FE  $J$  results at various points along the crack front ( $f=0, \pi/6, \pi/3$  and  $\pi/2$ ) with those from the proposed method.

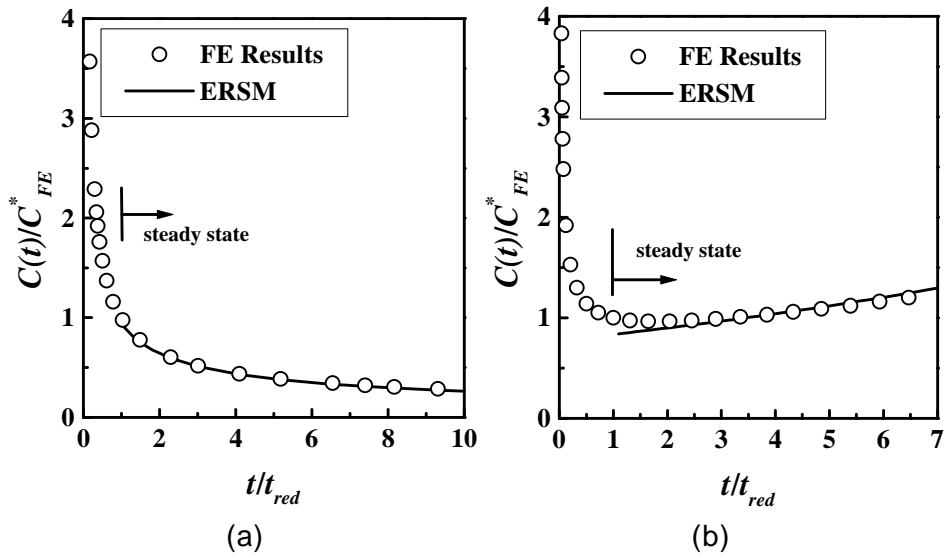


Fig. 10 Comparison of the FE  $C^*$  results with those from the proposed method for through-wall cracked pipes: (a) under global bending,  $q/p=0.4$ , RCC-MR law, and (b) under internal pressure,  $q/p=0.125$ ,  $q$ -projection law.

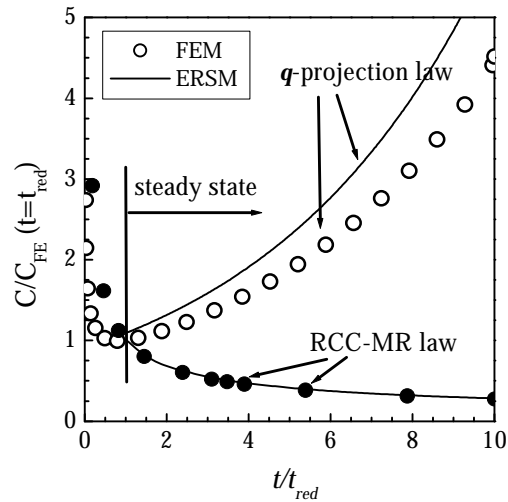


Fig. 11 Comparison of the FE  $C^*$  results with those from the proposed method for surface cracked pipes under pressure with  $a/t=0.5$  and  $b/p=0.4$ .